Surface Chemistry

International Edition: DOI: 10.1002/anie.201709029
German Edition: DOI: 10.1002/ange.201709029

Localized Supramolecular Peptide Self-Assembly Directed by Enzyme-Induced Proton Gradients

Jennifer Rodon Fores, Miguel Leonardo Martinez Mendez, Xiyu Mao, Déborah Wagner, Marc Schmutz, Morgane Rabineau, Philippe Lavalle, Pierre Schaaf, Fouzia Boulmedais, and Loïc Jierry**

Abstract: *Electrodes are ideal substrates for surface localized self-assembly processes. Spatiotemporal control over such processes is generally directed through the release of ions generated by redox reactions occurring specifically at the electrode. The so-used gradients of ions proved their effectiveness over the last decade but are in essence limited to material-based electrodes, considerably reducing the scope of applications. Herein is described a strategy to enzymatically generate proton gradients from non-conductive surfaces. In the presence of oxygen, immobilization of glucose oxidase (GOx) on a multilayer film provides a flow of protons through enzymatic oxidation of glucose by GOx. The confined acidic environment located at the solid–liquid interface allows the self-assembly of Fmoc-AA-OH (Fmoc = fluorenylmethyloxycarbonyl and A = alanine) dipeptides into β-sheet nanofibers exclusively from and near the surface. In the absence of oxygen, a multilayer nanoreactor containing GOx and horseradish peroxidase (HRP) similarly induces Fmoc-AA-OH self-assembly.*

Self-assembly is an easy and powerful way to organize matter from the molecular to the nanometer scale and beyond.[1] Spatial and temporal control over the self-assembly process has allowed the emergence of materials with original features through the design of nanostructured coatings or materials giving rise to a large scope of applications.[2,3] Currently, several methods describe the directed initiation and growth of supramolecular self-assembly at an interface. Most of them are triggered by a physical external stimulus or due to a template effect coming from a prior surface treatment of the material. Recent investigations based on chemical gradients have demonstrated a great potential 1) to localize precisely in space the molecular buildup,[4] 2) to control the assembly evolution over time,[5] and 3) to orientate the resulting nanostructure according to the features of one or several gradients.[6] This approach is inspired from reaction-diffusion processes found in Nature and appears as a promising way for further development of more complex chemical systems.[7]

Among the different gradient entities studied, protons are the most used because of their easy generation at a surface electrode. Indeed, oxidizing water or hydroquinone for instance leads to the production of protons that diffuse from the electrode to the surrounding environment, creating a confined acidic region at the interface. In 2010, Cameron's group described the surface-induced self-assembly of Fmoc protected dipeptides leading to the growth of a supramolecular hydrogel resulting in a dense fiber network.[8] Carbazole-protected amino acids have also been investigated for their spatially resolved self-assembly on electrode surfaces.[9] Using patterned electrodes, Payne demonstrated the specific control in space and time of the self-assembly of Fmoc protected phenylalanine by localized application of an electrical signal during a precise duration.[10] A fine electrochemical control of the proton production allowed the spatially and temporally resolved triggering of multicomponent hydrogels.[11] Surface-assisted self-assembly has also been used to developed efficient biosensors by immobilizing enzymes and bacteria.[12] Thus, the efficiency of this approach is well-established but the restriction to use electrodes as surfaces reduces considerably its range of applications. In the domain of surface-assisted self-assembly of low-molecular-weight hydrogelators (LMWH), only one alternative was described so far, based on the introduction of sulfonic acid groups on a surface catalyzing the in situ formation of the hydrogelator.[13]

Herein, we describe the self-assembly of peptides directed by a continuous gradient of protons produced enzymatically on a non-conductive surface. Our model system is composed of 1) Fmoc-AA-OH (Scheme 1a), a LMWH already described as hydrogelator under acidic conditions in solution[14,15] and 2) glucose oxidase (GOx), an enzyme producing protons through the transformation of glucose in gluconic acid in the presence of O_2 (Scheme 1b). Surface immobilization of GOx in a multilayer film will permit the production of protons in the presence of glucose. When Fmoc-AA-OH dipeptide diffuses toward the interface, its C-terminal carboxylate group is protonated, which should induce spontaneously its self-assembly solely at the interface (Scheme 1c). The buildup of GOx-coated surfaces and the evolution of the self-assembly process over time were followed both by quartz crystal microbalance (QCM-D) and attenuated total reflectance Fourier-transform infrared spectroscopy (ATR-FTIR).

[*] J. Rodon Fores, M. L. Martinez Mendez, X. Mao, D. Wagner, Dr. M. Schmutz, Prof. Dr. P. Schaaf, Dr. F. Boulmedais, Dr. L. Jierry
Université de Strasbourg, CNRS, Institut Charles Sadron (UPR22)
23 rue du Loess, BP 84047, 67034 Strasbourg Cedex 2 (France)
E-mail: schaaf@unistra.fr
loic.jierry@ics-cnrs.unistra.fr
Dr. M. Rabineau, Dr. P. Lavalle, Prof. Dr. P. Schaaf
Institut National de la Santé et de la Recherche Médicale, INSERM Unité 1121
11 rue Humann, 67085 Strasbourg Cedex (France)
and
Université de Strasbourg, Faculté de Chirurgie Dentaire
8 rue Sainte Elisabeth, 67000 Strasbourg (France)

Supporting information for this article can be found under: https://doi.org/10.1002/anie.201709029.

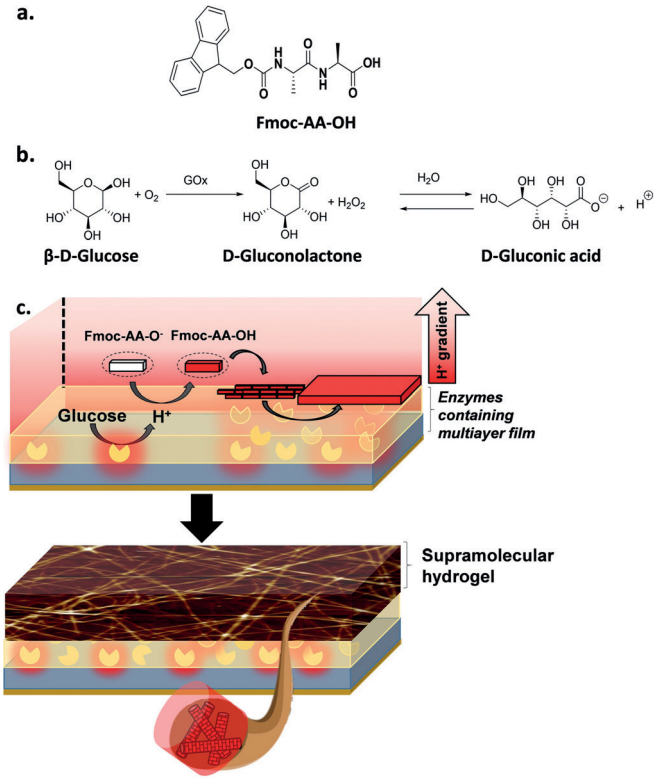

Scheme 1. a) Chemical structure of Fmoc-AA-OH dipeptide; b) enzymatic oxidation of glucose by GOx; c) enzymatically triggered self-assembly of peptides through proton gradient generation from a non-conductive surface onto which is adsorbed GOx.

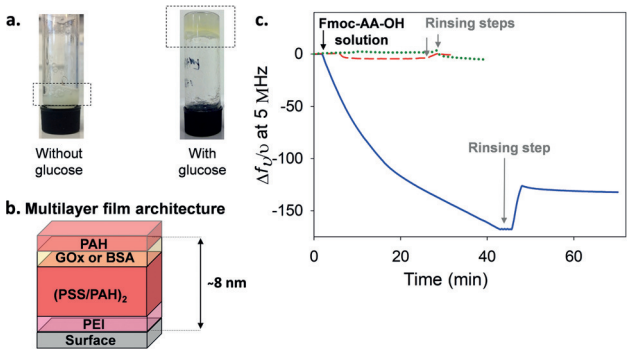

Figure 1. a) Upside-down vial gelation tests of Fmoc-AA-OH in the presence of GOx; b) architecture of $(GOx/PAH)_1$ and $(BSA/PAH)_1$ films; c) evolution of the normalized frequency shift (QCM-D) over time during the contact of Fmoc-AA-OH/glucose solution ($500\ \mu L\,min^{-1}$) with $(GOx/PAH)_1$ (blue line), with $(BSA/PAH)_1$ film (red dashed line) and during the contact of Fmoc-AA-OH solution (without glucose) with a $(GOx/PAH)_1$ film (green dotted line).

The morphology of the self-assembled architectures was investigated by atomic force microscopy (AFM), scanning electron microscopy (SEM), and cryo-SEM.

In solution, upside-down vial tests of Fmoc-AA-OH ($3.6\ mg\,mL^{-1}$) at different pH confirmed that gelation occurs in a few minutes at $pH \leq 4$ (Supporting Information, Figure S1). We have ensured that Fmoc-AA-OH ($3.6\ mg\,mL^{-1}$, pH 5) can effectively lead to hydrogel formation within roughly 10 min in the presence of GOx (6.25 μM) and glucose ($2\ mg\,mL^{-1}$, 11.10 mM) (Figure 1a). The isoelectric point (IP) of GOx is around 4.2. It can thus be electrostatically adsorbed onto a positively charged surface at pH 7. To immobilize GOx on a surface, we used the layer-by-layer technique based on the alternated deposition of polyanions and polycations on a surface,[16] a strategy already reported to design bioreactors.[17] We first modified the surface by dipping it into a solution of poly(ethylene imine) (PEI) and successively in poly(styrene sulfonate) (PSS) and poly(allylamine hydrochloride) (PAH) solutions to obtain a $PEI/(PSS/PAH)_2$ precursor multilayer film. GOx was then deposited and capped by a PAH layer to obtain the film $PEI/(PSS/PAH)_2/(GOx/PAH)_1$, named $(GOx/PAH)_1$ film. Its buildup was followed by QCM-D (Supporting Information, Figure S2) and its thickness was evaluated to about 8 nm (Supporting Information, Part 3). Its enzymatic activity was confirmed by spectrophotometric tests (Supporting Information, Figure S3).

When a $(GOx/PAH)_1$ film was put in contact with a Fmoc-AA-OH/glucose solution under a flow rate of $500\ \mu L\,min^{-1}$, an important decrease of the normalized frequency shift was observed by QCM-D over time, indicating a deposition of mass (Figure 1c). After 40 min, the solution was replaced by the buffer solution (rinsing step) and the normalized frequency shift increased slightly until it stabilized at around −120 Hz. Furthermore, the dissipation value at 15 MHz was of the order of 40×10^{-6} in agreement with the formation of a hydrogel (Supporting Information, Figure S4). Replacing GOx in the multilayer film by bovine serum albumin (BSA, $Mw \approx 66$ kDa, IP 4.7 at 25 °C) or removing glucose from the Fmoc-AA-OH solution did not lead to any significant changes of the normalized frequency shift (Figure 1c). These control experiments highlight the crucial role of the enzymatic activity of GOx in the multilayer film to direct the localized self-assembly process of Fmoc-AA-OH through the generation of protons. To increase the enzymatic proton production, several layers of GOx alternated with PAH have been incorporated in the multilayer to obtain a $PEI/(PSS/PAH)_2/(GOx/PAH)_n$, film named $(GOx/PAH)_n$, with $n = 2$, 3, and 6. When a Fmoc-AA-OH/glucose solution was put in contact with each of these films, a higher decrease of the normalized frequency shift was observed in comparison to $(GOx/PAH)_1$ film, indicating more deposited mass (Supporting Information, Figure S5). After 40 minutes of contact, the thickness reached about 1.1 μm, 2.3 μm, 3.2 μm, and 3.3 μm for self-assemblies induced by $(GOx/PAH)_1$, $(GOx/PAH)_2$, $(GOx/PAH)_3$, and $(GOx/PAH)_6$ films, respectively (Figure 2a). These thicknesses were obtained from the QCM data by using the Voinova model (Supporting Information, Part 3). Thus, the thickness of the self-assembled hydrogel increases with the number of GOx/PAH layers and levels off for $n > 3$. This is probably due to the limited diffusion of glucose into the multilayer for films exceeding 3 bilayers of GOx/PAH on the top.

Because glucose is the provider of protons through its oxidation by GOx, the influence of its concentration on the

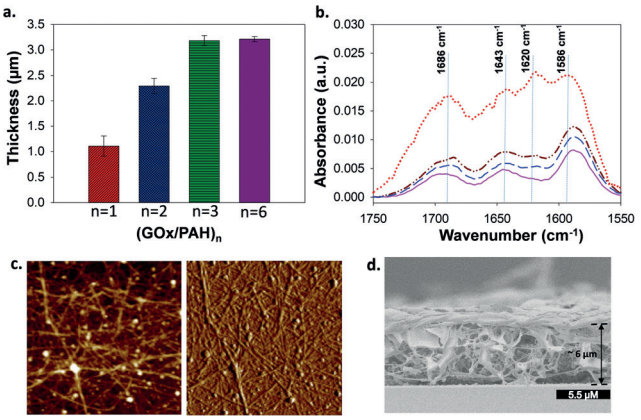

Figure 2. a) Thickness values of Fmoc-AA-OH self-assembly formed on $(GOx/PAH)_1$, $(GOx/PAH)_2$, $(GOx/PAH)_3$ and $(GOx/PAH)_6$ films. Standard deviations are calculated from three independent experiments; b) ATR-FTIR spectra of $(GOx/PAH)_3$ film in contact with Fmoc-AA-OH/glucose solution after 5 min (pink), 40 min (dashed blue), 1 h (dashed dot dotted brown), and 12 h (dotted red). These bands are visualized after subtraction of the spectra of $(GOx/PAH)_3$ film (Supporting Information, Figure S6); c) height and phase AFM images ($5.5 \times 5.5\ \mu m^2$) of Fmoc-AA-OH self-assembly (contact mode, dry state, *z*-scale 84 nm); d) cryo-SEM cross-section image of Fmoc-AA-OH self-assembly in the *z*-section.

self-assembly buildup was also investigated. Apart from the $2\ mg\,mL^{-1}$ concentration used up to now, we also studied the self-assembly process and gelation that occur in presence of 0.5, 1, 1.5, 3, 4, and $5\ mg\,mL^{-1}$ of glucose, keeping a constant concentration of Fmoc-AA-OH ($1\ mg\,mL^{-1}$). When brought in contact with a $(GOx/PAH)_3$ multilayer film, QCM-D monitoring showed no significant decrease of the frequency shift for concentrations lower than 2 mg mL, that is, 0.5, 1, and $1.5\ mg\,mL^{-1}$, despite the presence of few fibers as observed by SEM (Supporting Information, Figure S7 a–c). This means that the self-assembly can occur at these low concentrations of glucose but no gelation starts. In contrast, an important and almost equivalent frequency shift is observed for each of the 3 higher glucose concentrations investigated. It thus appears that a critical concentration which lies between 1.5 and $2\ mg\,mL^{-1}$ is necessary to get the formation of a hydrogel layer on the surface (Supporting Information, Figure S7 c). Higher glucose concentrations do not lead to layers thicker than the circa 3.2 µm obtained with $2\ mg\,mL^{-1}$. Furthermore, we also observed that the diameter of the smaller peptide fibers observed by SEM is roughly 55 nm whatever the glucose concentration used (Supporting Information, Figure S7 d).

To confirm the self-assembly of Fmoc-AA-OH, ATR-FTIR experiments were performed during the contact of Fmoc-AA-OH/glucose solution with $(GOx/PAH)_3$ films built on a ZnSe crystal. When bringing the peptide/glucose solution in contact with the surface, an increase in intensity of the amide I band region over time was observed. In particular, three vibration bands at 1686, 1643, and $1620\ cm^{-1}$ appear (Figure 2 b). The band at $1620\ cm^{-1}$ confirms a β-sheet structure adopted by the self-assembly of Fmoc-AA-OH. Furthermore, the presence of the band at $1686\ cm^{-1}$ allows the assignment of the antiparallel β-sheet conformation, which is consistent with observations done on other peptide-based supramolecular hydrogels.[18] The band at $1643\ cm^{-1}$ is characteristic of an amide band involved in polyproline II (PPII) conformation.[14a] The band located at $1586\ cm^{-1}$, and the peak area between 1750–1700 cm^{-1} can be attributed to COO^- antisymmetric stretch and C=O stretching of COOH of gluconic acid Fmoc-AA-OH, respectively. One observes a steady increase of the intensity of these bands over time during at least 12 hours, confirming the gradual buildup of the self-assembled layer. When GOx is replaced by BSA in the multilayer, no formation of Fmoc-AA-OH hydrogel is observed by ATR-FTIR (Supporting Information, Figure S8).

The morphology of the Fmoc-AA-OH self-assembly, obtained from $(GOx/PAH)_n$ films ($n = 1,3$) after 40 min of contact with Fmoc-AA-OH/glucose solution, was imaged by AFM in contact mode in the dry state and by SEM. A network of long fibers extending up to several hundred nanometers was observed that underpin the hydrogel structure (Supporting Information, Figure S9). This fibrous network is denser than the one obtained from $(GOx/PAH)_1$ film (Figure 2 c; Supporting Information, Figure S10). To visualize the internal morphology of the localized self-assembly, a $(GOx/PAH)_3$ functionalized glass surface was put into contact with a Fmoc-AA-OH/glucose solution for 16 h, rinsed, and imaged by cryo-SEM. The cross-section image shows the presence of an architecture of about 6 µm in thickness all along the glass surface (Figure 2 d), highlighting the full covering of the substrate by the self-assembled hydrogel and showing a regular thickness all along the surface (Supporting Information, Figure S11). It can be pointed that QCM and cryo-MEB indicate layer thicknesses exceeding several micrometers even if the absolute values differ by a factor of two. This may be due to the model used to treat the QCM data. We also verified that when a $(GOx/PAH)_3$ film is adsorbed on a specific area of the glass and this substrate is entirely brought in contact with the glucose and Fmoc-AA-OH mixture, the resulting hydrogel is formed strictly in the area pre-coated by the multilayer film. Only some peptide based fibers have spread over several micrometers at the interface between the multilayer area and the naked glass (Supporting Information, Figure S12).

It must be noted that a slight flow ($500\ \mu L\,min^{-1}$) of Fmoc-AA-OH/glucose was necessary for the self-assembly process to occur: only a low QCM signal was observed when the mixture was in contact with $(GOx/PAH)_3$ film without flow (Figure 3 b). This can be explained by the fact that GOx requires a supply in O_2 to be effective, continuously brought by the flow of reactants. When Fmoc-AA-OH/glucose solution was degassed and injected with a similar flow rate, no decrease of the fundamental frequency shift was observed confirming this hypothesis (Supporting Information, Figure S13). To provide the in situ fuel, that is, O_2, to the system without flow of the reactants, a second enzyme, the horseradish peroxidase (HRP), was added onto the multilayer film. This enzyme can transform H_2O_2, produced when glucose is reduced by GOx, into O_2 (Figure 3 a).[19] With respect to the IP 8.8 of HRP, the following multilayer has been investigated $PEI/(PSS/PAH)_2/GOx/PAH/PSS/HRP$. Unfortu-

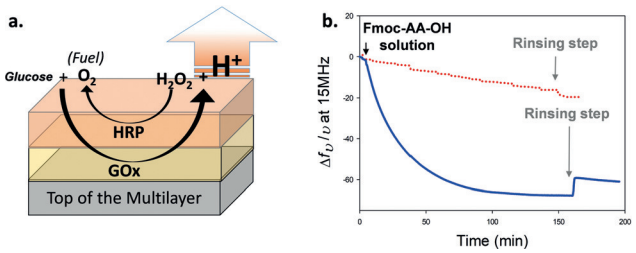

Figure 3. a) Enzymatically triggered proton gradient generated from $(GOx/HRP)_1$ film; b) evolution of the normalized frequency shift (QCM-D) over time when $(GOx/PAH)_3$ film (red dotted line) and (GOx/HRP) film (blue line) are brought in contact with Fmoc-AA-OH/glucose without flow.

nately, when this film was brought in contact with Fmoc-AA-OH and glucose, no self-assembly was observed (Supporting Information, Figure S14). The efficiency of this system is sensitive to the spatial distance between the two enzymes: the optimal motor can be effectively designed when both enzymes are spatially very close together.[20] Thus HRP was directly adsorbed onto GOx leading to the following multilayer $PEI/(PSS/PAH)_2/(GOx/HRP)$ named (GOx/HRP). When this film was brought in contact with a Fmoc-AA-OH/glucose without flow, a decrease of the normalized frequency shift was measured showing the self-assembly of Fmoc-AA-OH (Figure 3b) which was confirmed by ATR-FTIR and AFM experiments (Supporting Information, Figures S15 and S16).

In summary, despite recent developments of enzyme-assisted self-assembly strategies no approach has been reported involving enzyme-immobilized surfaces to create a flow of ions at an interface to initiate a self-assembly process. Herein, we present a first enzymatic system based on GOx to produce protons which trigger the self-assembly of an Fmoc-AA-OH peptide network. It requires the presence of O_2 in solution. We also show that the simultaneous presence of GOx and HRP on top of the multilayer allows circumventing the outside supply of O_2 through a cascade of reactions. Using this strategy allows getting rid of conductive substrates to realize proton-gradient-induced self-assemblies and thus to generalize this type of self-assembly to almost any kind of substrate, whatever its nature and geometry. Such multi-enzymatic systems localized on surfaces lead to molecular motors that can tune 1) the self-assembly process, 2) its resulting function, 3) its sensitivity/responsivity to surrounding stimuli, and finally 4) its evolution over space and time. This approach is still in its infancy but represents an exciting perspective for further research.

Acknowledgements

Maëlle Cahu and Camille Damestoy are acknowledged for technical help. We gratefully acknowledge the financial support from Agence Nationale de la Recherche (ANR-15-CE29-0015-02), International Center for Frontier Research in Chemistry (icFRC), Labex "Chimie des Systèmes Complexes" (Labex CSC, PSC-016), University of Strasbourg Institute for Advanced Study (USIAS) and Institut Universitaire de France (IUF).

Conflict of interest

The authors declare no conflict of interest.

Keywords: coating · nanostructures · self-assembly · supramolecular chemistry · surface chemistry

How to cite: *Angew. Chem. Int. Ed.* **2017**, *56*, 15984–15988
Angew. Chem. **2017**, *129*, 16200–16204

[1] a) J.-M. Lehn in *Supramolecular Chemistry*, Wiley-VCH, Weinheim, **1995**; b) G. M. Whitesides, B. Grzybowski, *Science* **2002**, *295*, 2418–2421; c) T. Aida, E. W. Meijer, S. I. Stupp, *Science* **2012**, *335*, 813–817.
[2] a) M. A. Cohen Stuart, W. T. S. Huck, J. Genzer, M. Müller, C. Ober, M. Stamm, G. B. Sukhorukov, I. Szleifer, V. V. Tsukruk, M. Urban, F. Winnik, S. Zauscher, I. Luzinov, S. Minko, *Nat. Mater.* **2010**, *9*, 101–103; b) K. Ariga, Q. Ji, W. Nakanishi, J. P. Hill, M. Aono, *Mater. Horiz.* **2015**, *2*, 406–413.
[3] a) M. Komiyama, K. Yoshimoto, M. Sisido, K. Ariga, *Bull. Chem. Soc. Jpn.* **2017**, *90*, 967–1004; b) N. Singh, M. Kumar, J. F. Miravet, R. V. Ulijn, B. Escuder, *Chem. Eur. J.* **2017**, *23*, 981–993.
[4] A. Dochter, T. Garnier, E. Pardieu, N. T. T. Chau, C. Maerten, B. Senger, P. Schaaf, L. Jierry, F. Boulmedais, *Langmuir* **2015**, *31*, 10208–10214.
[5] C. Vigier-Carrière, T. Garnier, D. Wagner, P. Lavalle, M. Rabineau, J. Hemmerlé, B. Senger, P. Schaaf, F. Boulmedais, L. Jierry, *Angew. Chem. Int. Ed.* **2015**, *54*, 10198–10201; *Angew. Chem.* **2015**, *127*, 10336–10339.
[6] R. M. Capito, H. S. Azevedo, Y. S. Velichko, A. Mata, S. I. Stupp, *Science* **2008**, *319*, 1812–1816.
[7] a) S. Soh, M. Byrska, K. Kandere-Grzybowska, B. A. Grzybowski, *Angew. Chem. Int. Ed.* **2010**, *49*, 4170–4198; *Angew. Chem.* **2010**, *122*, 4264–4294; b) G. N. Pandian, H. Sugiyama, *Bull. Chem. Soc. Jpn.* **2016**, *89*, 843–868.
[8] E. K. Johnson, D. J. Adams, P. J. Cameron, *J. Am. Chem. Soc.* **2010**, *132*, 5130–5136.
[9] P. S. Kubiak, S. Awhida, C. Hotchen, W. Deng, B. Alston, T. O. McDonald, D. J. Adams, P. J. Cameron, *Chem. Commun.* **2015**, *51*, 10427–10430.
[10] Y. Liu, E. Kim, R. V. Ulijn, W. E. Bentley, G. F. Payne, *Adv. Funct. Mater.* **2011**, *21*, 1575–1580.
[11] J. Raeburn, B. Alston, J. Kroeger, T. O. McDonald, J. R. Howse, P. J. Cameron, D. J. Adams, *Mater. Horiz.* **2014**, *1*, 241–246.
[12] Y. Liu, J. L. Terrel, C. Y. Tsao, H. C. Wu, V. Javvaji, E. Kim, Y. Cheng, Y. Wang, R. V. Ulijn, S. R. Raghavan, G. W. Rubloff, W. E. Bentley, G. F. Payne, *Adv. Funct. Mater.* **2012**, *22*, 3004–3012.
[13] A. G. L. Olive, N. H. Abdullah, I. Ziemecka, E. Mendes, R. Eelkema, J. H. van Esch, *Angew. Chem. Int. Ed.* **2014**, *53*, 4132–4136; *Angew. Chem.* **2014**, *126*, 4216–4220.
[14] a) X. Mu, K. M. Eckes, M. M. Nguyen, L. J. Suggs, P. Ren, *Biomacromolecules* **2012**, *13*, 3562–3571; b) V. Jayawarna, M. Ali, T. A. Jowitt, A. F. Miller, A. Saiani, J. E. Gough, R. V. Ulijn, *Adv. Mater.* **2006**, *18*, 611–614; c) D. J. Adams, L. M. Mullen, M. Berta, L. Chen, W. J. Frith, *Soft Matter* **2010**, *6*, 1971–1980.
[15] W. Cheng, Y. Li, *Sci. China Phys. Mech. Astron.* **2016**, *59*, 678711.
[16] G. Decher, *Science* **1997**, *277*, 1232–1237.
[17] a) M. Onda, Y. Lvov, K. Ariga, T. Kunitake, *Biotechnol. Bioeng.* **1996**, *51*, 163–167; b) M. Onda, Y. Lvov, K. Ariga, T. Kunitake, *J. Ferment. Bioeng.* **1996**, *82*, 502–506; c) S. Zhang, S. Demoustier-

Champagne, A. M. Jonas, *Biomacromolecules* **2015**, *16*, 2382 – 2393.
[18] N. Yamada, K. Ariga, M. Naito, K. Matsubara, E. Koyama, *J. Am. Chem. Soc.* **1998**, *120*, 12192 – 12199.
[19] J. Hernández-Ruiz, M. B. Arnao, A. N. P. Hiner, F. Garcia-Canovas, M. Acosta, *Biochem. J.* **2001**, *354*, 107 – 114.
[20] L. Xin, C. Zhou, Z. Yang, D. Liu, *Small* **2013**, *9*, 3088 – 3091.

Manuscript received: September 1, 2017
Revised manuscript received: October 11, 2017
Accepted manuscript online: October 23, 2017
Version of record online: November 15, 2017

